CrystEngComm

Accepted Manuscript

This is an *Accepted Manuscript*, which has been through the Royal Society of Chemistry peer review process and has been accepted for publication.

Accepted Manuscripts are published online shortly after acceptance, before technical editing, formatting and proof reading. Using this free service, authors can make their results available to the community, in citable form, before we publish the edited article. We will replace this *Accepted Manuscript* with the edited and formatted *Advance Article* as soon as it is available.

You can find more information about *Accepted Manuscripts* in the Information for Authors.

Please note that technical editing may introduce minor changes to the text and/or graphics, which may alter content. The journal's standard Terms & Conditions and the Ethical guidelines still apply. In no event shall the Royal Society of Chemistry be held responsible for any errors or omissions in this *Accepted Manuscript* or any consequences arising from the use of any information it contains.

ROYAL SOCIETY OF CHEMISTRY

www.rsc.org/crystengcomm

Table of contents

Design and Syntheses of Hybrid Supramolecular Architectures: Based on $[Fe(C_2O_4)_3]^{3-}$ Metallotectons and Diverse Organic Cations

Lei Wang [a*], Wenqiang Wang [a], Dong Guo [a], Ao Zhang [a], Yaoguang Song [a], Yiheng Zhang [a], and Keke Huang [b*]

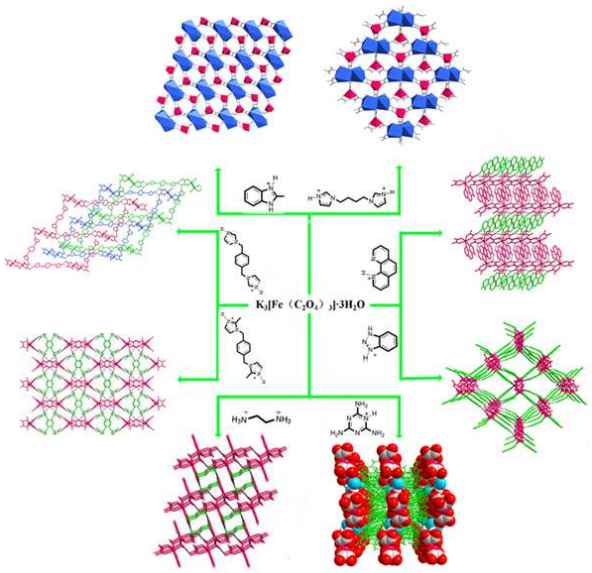

Employing $[Fe(C_2O_4)_3]^{3-}$ ($C_2O_4^{2-}$ = oxalate) metallotectons as building unit, a series of 3D iron-organic compounds were synthesized and characterized by single-crystal X-ray diffraction, IR and TGA.

CrystEngComm Accepted Manuscript

CrystEngComm RSCPublishing

ARTICLE

Design and Syntheses of Hybrid Supramolecular Architectures: Based on $[Fe(C_2O_4)_3]^{3-}$ Metallotectons and Diverse Organic Cations

Cite this: DOI: 10.1039/x0xx00000x

Received 00th January 2012,
Accepted 00th January 2012

DOI: 10.1039/x0xx00000x

www.rsc.org/

Lei Wang [a*], Wenqiang Wang [a], Dong Guo [a], Ao Zhang [a], Yaoguang Song [a], Yiheng Zhang [a], and Keke Huang [b*]

Employing $[Fe(C_2O_4)_3]^{3-}$ ($C_2O_4^{2-}$ = oxalate) metallotectons as building units, a series of 3D iron-organic compounds with formulas $[K(H\text{-}L_1)_2\{Fe(C_2O_4)_3\}\cdot 2H_2O]$ **1,** $[(H\text{-}Phen)\{Fe(C_2O_4)_2\}(Phen)\cdot 3H_2O]$ **2**, $[(H_2\text{-}L_2)_2\{Fe_2(C_2O_4)_3Cl_4\}]$ **3**, $[K(H_2L_3)\{Fe(C_2O_4)_3\}\cdot 2H_2O]$ **4**, $[K(H_2\text{-}L_4)\{Fe(C_2O_4)_3\}\cdot H_2O]$ **5**, $[(H\text{-}L_5)\{Fe(C_2O_4)(L_5)\}]$ **6**, $[(H_2\text{-}L_6)_2\{Fe_2(C_2O_4)_4(OH)_2\}\cdot 2H_2O]$ **7**, $[(H\text{-}L_7)_4\{Fe(C_2O_4)_3\}Cl\cdot 2H_2O]$ **8** (with L_1 = 2-methylbenzimidazole, Phen = 1,10-phenanthroline, L_2 = 1,4-bis(imidazol-1-ylmethyl)benzene, L_3 = 1,4-bis((2-Methylimidazol-1-yl)methyl)benzene, L_4 = 1,1'-Butane-1,4-diylbis(1H-imidazole), H-L_5 = 1H-benzotriazole, L_6 = 1,2-ethylenediamine, L_7 = melamine) have been synthesized and characterized by single-crystal X-ray diffraction. Compounds **1** and **5** possess different 2D $[KFe(C_2O_4)_3]^{2-}$ layers. Compound **2** features a 2D hydrogen bonded networks completed by trimer water clusters and $[Fe(C_2O_4)_2(Phen)]^-$ anions via hydrogen bonds. Compounds **3-6** feature a series of 2D layers, which are further extended into 3D supramolecular structure through C-H···O hydrogen bonds. Distinct $[Fe_2(C_2O_4)_3Cl_4]^{4-}$ unit and $[Fe_2(C_2O_4)_4(OH)_2]^{4-}$ unit are showed in compounds **3** and **7**, respectively. Trinary hydrogen bonds and doubly hydrogen bonds are simultaneously displayed in **8** as well as the N-H···Cl and O-H···Cl hydrogen bonds. Furthermore, in order to examine the thermal stability of all compounds, the TGA were carried out.

Introduction

One of the important missions of supramolecular chemistry is to make ordered molecular material with predetermined structure and property.[1-2] According to this line, to design single-crystalline solids with desired structures or potential applications, different kinds of molecular building blocks (inorganic, organometallic, or organic) have been rational utilized.[3] Meatl-organic coordination compounds as reactants provide not only transition metal ions but also segmental organic ligands or templates in synthesis systems.[4-5] Qiu's group by uning $Cd(phen)_2(NO_3)_2$ as the metal source, prepared a series of 3D supramolecular framework.[6] And it is demonstrated that novel topologies can be obtained by using a meatl-organic coordination compound as the starting material. By using a racemic mix of chiral $[Co(dien)_2]Cl_3$ complex as the template, an interesting open-framework zinc phosphate $[Zn_2(HPO_4)_4][Co(dien)_2]\cdot H_2O$ has been prepared with multidirectional helical channels by Yu's group.[7] The rigid octahedrally $[Co(dien)_2]^{3+}$ is chiral, which exists as both the △ and ∧ enantiomers. Their work demonstrated that the chiral inorganic structural motif can be induced by the chiral coordination complex template.

Recently, Jean and co-workers fabricated a series of nanoporous architectures by using $[Zr(C_2O_4)_4]^{4-}$ ($C_2O_4^{2-}$ = oxalate) as building blocks linked with M^{2+} metal ions via coordinative covalent bonding.[8] Futhermore, by introducing linear flexible or V-shaped organic cations into the reaction system with $[Zr(C_2O_4)_4]^{4-}$metallotectons via hydrogen bonds, they designed and synthesized four supramolecular materials with porous frameworks.[9] Jean's work demonstrated that meatl-organic coordination compounds are easy able to engage in well identified and multiple intermolecular interactions, and connect metal ions via coordinative covalent bonding or other organic ligands via hydrogen bonds.[10] Along this route, we pay special attention to the possibility of using $[Fe(C_2O_4)_3]^{3-}$ as building-

[a] College of Chemistry and Molecular Engineering, Qingdao University of Science and Technology, Qingdao 266042, P. R. China. E-mail: inorchemwl@126.com; Fax: (+86) 532-840-22681
[b] State Key Laboratory of Inorganic Synthesis and Preparative Chemistry, Jilin University, Changchun, 130012, PR China. E-mail:kkhuang@jlu.edu.cn;

† Electronic Supplementary Information (ESI) available: IR, and TGA data. CCDC reference numbers 983359-983366. For ESI and crystallographic data in CIF or other electronic format see DOI:XXXXXXXXX

CrystEngComm Accepted Manuscript

block to design 3D hybrid supramolecular architectures. Relative to organic molecules, the six outer oxygen atoms of the $[Fe(C_2O_4)_3]^{3-}$ units not only can connect metal ions, but also act as efficient hydrogen-bond acceptors in supramolecular structures, generating heterometallic frameworks or new H-bonded networks.[11-14] Moreover, compared with the stability of $[Zr(C_2O_4)_4]^{4-}$, $[Fe(C_2O_4)_3]^{3-}$ can be seen as a more fascinating candidate to assemble various crystalline architectures for the follow two interesting characters. (i) In aqueous solution at low pH, the aquation reaction of $K_3[Fe(C_2O_4)_3]\cdot 3H_2O$ will firstly take place, giving rise to $[Fe(C_2O_4)_2\cdot(H_2O)_2]^-$ anion, which is easy to lose water molecules in the presence of secondary ligand.[15] (ii)The changeable number of replaced oxalate groups and potassium atoms from starting materials of $K_3[Fe(C_2O_4)_3]\cdot 3H_2O$, could change the behavior of node resulting in various H-bonded architectures. To date, $K_3[Fe(C_2O_4)_3]\cdot 3H_2O$ have been used to fabricate functional metal-organic frameworks and nanostructured materials; however, utilizing $[Fe(C_2O_4)_3]^{3-}$ as metallotectons linked with N-donor ligands to construct hybrid supramolecular frameworks is rare.[15-18] Thus, our research interest focus on such system for combining protonated nitrogen-containing ligands with the building-block of $[Fe(C_2O_4)_3]^{3-}$ anion. Herein, we present a series of 3D hybrid supramolecular materials based on $[Fe(C_2O_4)_3]^{3-}$ metallotectons and diverse organic cations (see Scheme 1). These organic cations not only act as H-bonded donors, but also act as bridges between two $[Fe(C_2O_4)_3]^{3-}$ metallotectons to afford H-bonded frameworks by means of H-bonds.

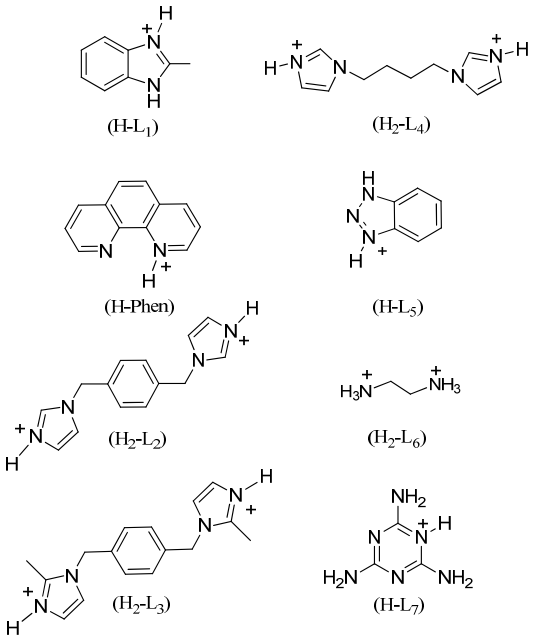

Scheme 1 N-donor Liands Used in This Work

Experimental section

General materials and methods

All staring chemicals for synthesis were commercially available sources and used without any further purification. Elemental analyses were performed on a Perkin-Elmer 2400 elemental analyzer. Fourier transform infrared (FT-IR) spectra were recorded with a Nicolet Impact 410 FTIR spectrometer by KBr pellets in the range 4000–400 cm^{-1}. Thermogravimetric analysis (TGA) experiments were completed on a Perkin-Elmer TGA 7 thermogravimetric analyzer at a heating rate of 10 °C min^{-1} in N_2 atmosphere.

Synthesis of $[K(H\text{-}L_1)_2\{Fe(C_2O_4)_3\}\cdot 2H_2O]$ (1). An aqueous solution (3 mL, pH ≈ 2 with diluted HCl) of 2-methylbenzimidazole (47.6mg, 0.4mmol) was slowly added to 3mL aqueous solution of $\{K_3[Fe(C_2O_4)_3]\cdot 3H_2O\}$ (197mg, 0.4 mmol,), then 4 mL ethanol was added to the resulting solution with constant stirring for 5 minutes. After two hours emerald block crystals were obtained at room temperature. The crystals were filtered and washed with water solution, then dried in air. Yield: 86%. Anal. Calcd for $C_{22}H_{22}FeKN_4O_{14}$ (%):C 39.92, H 3.33, N 8.47. Found: C 39.73, H 3.42, N 8.59. IR (KBr): v(cm^{-1}) = 3485 (m), 3274 (m), 3058 (m), 2925 (m), 2850 (m), 2757 (m), 2656 (m), 1709(s), 1692 (s), 1628 (s), 1579 (m), 1466 (m), 1430 (m), 1384 (s), 1288 (m), 1250(m), 1223(m), 1023 (w), 975 (w), 893 (w), 806 (w), 768 (w), 625 (w), 503 (w).

Synthesis of $[(H\text{-}Phen)\{Fe(C_2O_4)_2(Phen)\}\cdot 3H_2O]$ (2). The single crystals are obtained by slow interdiffusion in a test tube of an aqueous solution of $\{K_3[Fe(C_2O_4)_3]\cdot 3H_2O\}$(197 mg, 0.4 mmol, 4.5 mL as bottom solution), EtOH/H2O = 4.5 ml/3 ml as interlayer and a mixed solution of EtOH/H_2O = 3mL/1mL (pH ≈ 1-2 with diluted HCl) of 1,10-phenanthroline hydrate (159 mg, 0.8 mmol, as upper layer) in dark environment. After four months one red block crystal was obtained at room temperature. The obtained crystal was filtered and washed with ethanol-water solution (v/v = 1/1), and dried in vacuum desiccators. Yield: 15%. Anal. Calcd for $C_{28}H_{23}FeN_4O_{11}$ (%): C 51.90,H 3.55,N 8.65. Found: C 51.74, H 3.66, N 8.74. IR (KBr): v(cm^{-1}) = 3425 (m), 3036 (w), 1707 (m), 1665 (s), 1579(m), 1424(m), 1404 (m), 1383 (s), 1266 (m), 1258 (m), 1206 (m), 1137(w), 1096(w), 872 (m), 789 (m), 728 (m), 536(m).

Synthesis of $[(H_2\text{-}L_2)_2\{Fe(C_2O_4)_{1.5}Cl_2\}_2]$ (3). A mixed solution (H_2O/EtOH = 3mL/4mL, pH ≈ 2 with diluted HCl) of L_2 (274mg, 1mmol) was slowly added to 3mL water solution of $\{K_3[Fe(C_2O_4)_3]\cdot 3H_2O\}$ (491mg, 1mmol) under continuous stirring. The resulting solution was kept for slow evaporation at room temperature. Light brown block crystals were obtained after two months. The obtained crystals were separated from the mother liquor by filtration, washed with water solution, and dried in air. Yield: 75%. Anal. Calcd. for $C_{34}H_{32}Cl_4Fe_2N_8O_{12}$ (%):C 40.87, H 3.21 ,N 11.22. Found: C 40.64, H 3.32, N 11.36. IR (KBr): v(cm^{-1}) = 3431 (m), 3139 (m), 2921 (m), 2851 (m), 1706 (m), 1682 (s), 1648 (s),1605 (m), 1543 (m), 1430 (m), 1414 (m), 1303 (w), 1271 (m), 1083 (w), 1015 (w),843 (w), 801 (w), 768 (w), 622 (w).

Synthesis of $[K(H_2\text{-}L_3)\{Fe(C_2O_4)_3\}\cdot 2H_2O]$ (4). This compound was prepared according to the methodology described for **1**, reacting the same amount of $\{K_3[Fe(C_2O_4)_3]\cdot 3H_2O\}$ with 1 equiv of L_3 (120.8mg, 0.4 mmol) in the same water and ethanol volume, and under comparable pH conditions. Yield: 45%. Anal. Calcd for (%):C 26.58, H 3.62, N 8.44. Found: C 26.39, H 3.75, N 8.62. IR (KBr): v(cm^{-1}) = 3442 (m), 3135 (m), 2920 (m), 2851 (m), 1691 (s), 1645 (s), 1597

CrystEngComm Accepted Manuscript

This journal is © The Royal Society of Chemistry 2012

(m), 1526 (w), 1427 (m), 1351 (w), 1309 (w), 1273 (m), 1115 (w), 870 (w), 799 (m), 783 (m), 759 (w), 742 (m), 479 (w).

Synthesis of [K(H_2-L_4){Fe(C_2O_4)$_3$}·H_2O] (5). 3 ml aqueous solution (pH ≈ 2 with diluted HCl) of L_4 (152mg, 0.8mmol) was mixed to 3ml water solution of {K_3[Fe(C_2O_4)$_3$]·3H_2O} (197mg, 0.4 mol,), and the resulting solution was stirred for 15 min and kept for slow evaporation at room temperature. Emerald block crystals were gained after one week. The obtained crystals were filtered and dried in air. Yield: 43%. Anal. Calcd for $C_{16}H_{18}FeKN_4O_{13}$ (%):C 33.73, H 3.16, N 9.84. Found: C 33.54, H 3.28, N 3.98. IR (KBr): ν(cm^{-1}) = 3475 (m), 3131 (m), 2920 (w) 2850 (w), 1711 (m), 1670 (s), 1569 (w), 1396 (m), 1308 (w), 1280 (w), 1257 (w), 890 (w), 802 (w), 497(w).

Synthesis of [(H-L_5){Fe(C_2O_4)(L_5)}] (6). The same synthetic methodology as for **5** was used except that L_4 was replaced by 1H-benzotriazole and 3mL aqueous solution of {K_3[Fe(C_2O_4)$_3$]·3H_2O} was revised as 6mL aqueous solution. Red long striped crystals were obtained after one week. The obtained crystals were filtered and dried in air. Yield: 72%. Anal. Calcd for $C_{14}H_9FeN_6O_4$ (%):C 44.08, H 2.36, N 22.04. Found: C 43.86, H 2.49, N 22.23. IR (KBr): ν(cm^{-1}) = 3441 (m), 3136 (m), 3095 (m), 2995 (m), 2995 (m), 2959 (m), 2906 (m), 2861 (w), 1674 (s), 1616 (s), 1458 (w), 1419 (w), 1356(w), 1313(s), 1221(m), 1113(m), 1025(m), 908 (w), 855 (w), 841 (w), 794 (m), 788 (m), 748 (s), 487 (w), 428 (w).

Synthesis of [(H_2-L_6)$_2$Fe(C_2O_4)$_2$(OH)}$_2$·2H_2O] (7). Ethylenediamine dihydrochloride (333 mg, 0.4 mmol) was dissolved in 3 ml water solution and 3 ml aqueous solution of {K_3[Fe(C_2O_4)$_3$]·3H_2O} (197 mg, 0.4 mmol) was added to this solution, then ethanol (4 mL) was added to the resulting solution with stirring for 10 minutes. Slow evaporation of the final solution, in dark environment, resulted in the formation of emerald crystals of **7** (Yield: 20%), which are filtered and dried in air. Anal. Calcd for $C_{12}H_{26}Fe_2N_4O_{20}$ (%): C 21.88, H 3.95, N 8.51. Found: C 21.65, H 4.08, N 8.65. IR (KBr): ν(cm^{-1}) = .3437 (m), 3199 (m), 2920(m), 1713 (s), 1778 (s), 1522 (w), 1425 (m), 1390 (m), 1330 (w), 1288 (w), 1252 (w), 1101 (w), 1051 (w), 1015 (w), 900 (w), 799 (m), 785 (m), 532 (w), 494 (w), 467 (w).

Synthesis of [(H-L_7)$_4$Fe(C_2O_4)$_3$}Cl·2H_2O] (8). This compound was prepared according to the methodology described for **6**, reacting the same amount of {K_3[Fe(C_2O_4)$_3$]·3H_2O} with 2 equiv of L_7 (100.8 mg, 0.8 mmol) in the same water volume, and under comparable pH conditions. Yield: 45%. Anal. Calcd for $C_{18}H_{32}ClFeN_{24}O_{14}$ (%):C 24.00 ,H 3.56, N 37.33. Found: C 23.79, H 3.67, N 37.48. IR (KBr): ν(cm^{-1}) = 3391 (m), 3246 (m), 3096 (m), 2698 (w), 1734 (m), 1693 (s), 1507 (m), 1386 (m), 1277 (m), 1158 (w), 984 (w), 899 (w), 807 (m), 776 (m), 689 (w), 586 (m).

X-Ray crystallography

The diffraction data for compounds **1-8** were collected with a graphite monochromatic MoKa radiation (λ= 0.71073 Å) on a Siemens Smart CCD single-crystal X-ray diffractometer. All empirical absorption corrections were applied utilizing SADABS program. All structures were solved by direct methods using the SHELXS-97 program of the SHELXTL package and refined by full-matrix least-squares on F^2 SHELXL-97.[19] All non-hydrogen atoms in the eight structures were refined anisotropically. Further details for crystallographic data and structural refinement results of the compounds are given in **Table 1**, and selected H-bond lengths and angles are listed in Table S1 (Supporting Information).

Table 1 Crystal data and structure refinement summary for compounds **1-8**

Compound	**1**	**2**	**3**	**4**	**5**	**6**	**7**	**8**
formula	$C_{22}H_{22}FeKN_4O_{14}C_{28}H_{23}FeN_4O_{11}$	$C_{34}H_{32}Cl_4Fe_2N_8O_{12}$	$C_{22}H_{24}FeKN_4O_{14}$	$C_{16}H_{18}FeKN_4O_{13}$	$C_{14}H_9FeN_6O_4$	$C_{12}H_{26}Fe_2N_4O_{20}$	$C_{18}H_{32}ClFeN_{24}O_{14}$	
M	661.39	647.35	998.18	663.40	569.29	381.12	658.07	899.98
T, K	293	293	293	293	293	293	293	293
crystal system	orthorhombic	Triclinic	triclinic	monoclinic	monoclinic	monoclinic	triclinic	monoclinic
space group	Ccca	*P*$\bar{1}$	*P*$\bar{1}$	*C*2/c	*C*2/c	*Cc*	*P*$\bar{1}$	*P*2(1)/c
a, Å	13.4174(6)	7.5990(5)	10.6758(8)	14.7637(12)	14.7204(5)	14.5197(10)	7.6299(6)	11.597(4)
b, Å	18.1772(7)	11.7318(7)	10.7457(8)	20.5458(15)	16.3987(6)	12.4744(8)	8.1873(7)	22.299(7) A
c, Å	22.3340(8)	16.7071(10)	10.8774(9)	9.5211(8)	18.7939(7)	9.3796(7)	10.0309(9)	13.655(5) A
α, deg	90	88.5820(10)	113.219	90	90	90	107.527(8)	90
β, deg	90	88.2020(10)	109.138	107.412(9)	103.2590(10)	109.260(8)	100.261(7)	94.344(6)
γ, deg	90	71.4000(10)	99.294(6)	90	90	90	95.270(7)	90
V, Å^3	5447.1	1410.78	1020.84	2755.7	4415.8	1603.79	or	3521(2)
Z	8	2	1	4	8	4	2	4
ρ_{calcd} (g/cm^3)	1.613	1.524	1.624	1.599	1.713	1.578	1.881	1.698
μ(mm^{-1})	0.784	0.604	1.043	0.775	0.949	0.974	1.354	0.604
F(000)	2712	666	508	1364	2328	772	338	1852
R_{int}	0.0386	0.0614	0.0343	0.0133	0.0368	0.0346	0.0216	0.0711
Final R_1, wR_2 (all data)	0.0449, 0.1041	0.0435, 0.1298	0.0877, 0.1294	0.0315, 0.0801	0.0382, 0.0932	0.0492, 0.0921	0.0434, 0.0940	0.0502, 0.1497
GOF on F^2	1.043	1.013	1.020	1.030	1.093	1.012	1.065	0.993

[a] $R_1 = \Sigma||F_o| - |F_c||/\Sigma|F_o|$; wR_2[b] = $\{\Sigma[w(F_o^2-F_c^2)^2]/\Sigma[w(F_o^2)]^2\}^{1/2}$

Results and discussion

Syntheses The synthesis of the hybrid supramolecular materials described here have been performed by mixing an aqueous solution of K_3[Fe(C_2O_4)$_3$]·3H_2O with an acidic solution (pH ≈ 2) of the organic unit in two ratios (1:1 and 1:2). Crystallization of K_3[Fe(C_2O_4)$_3$]·3H_2O with 2-methylbenzimidazole (1:1), 1,10-phenanthroline (1:2), 1,4-bis(imidazol-1-ylmethyl)benzene (1:1),

CrystEngComm Accepted Manuscript

1,4-bis((2-Methylimidazol-1-yl)methyl)benzene (1:1), 1,1'-Butane-1,4-diylbis(1H-imidazole) (1:2), 1H-benzotriazole (1:2), 1,2-ethylenediamine (1:1), melamine (1:2) results in crystals. Crystalline samples were gained by slow evaporation or interdiffusion of the reagent solutions. The structure of building-block of $[Fe(C_2O_4)_3]^{3-}$ was changed in different experimental conditions, resulting in different kinds of H-bonded frameworks: Unchangeable structure of building-block: with 2-methylbenzimidazole (**1**), 1,4-bis((2-Methylimidazol-1-yl)methyl)benzene (**4**), 1,1'-Butane-1,4-diylbis(1H-imidazole) (**5**) and melamine (**8**); Changeable structure of building-block: with 1,10-phenanthroline (**2**), 1,4-bis(imidazol-1-ylmethyl)benzene (**3**), 1H-benzotriazole (**6**) and 1,2-ethylenediamine (**7**). The schematic representation of structural evolution of building-block was summarized in **Scheme 2**. In our later exploratory reactions, compounds **1,** 4, and **5** can be obtained in acidulated solution (pH ≈ 2 with HNO_3). However, other compounds can't be obtained. This result suggests that different inorganic acids also affect the H-bonded topology.

Scheme 2. Coordination Modes of $C_2O_4^{2-}$ in Complexes **1-8**. (Color scheme: carbon, gray; oxygen, red; metal, blue.)

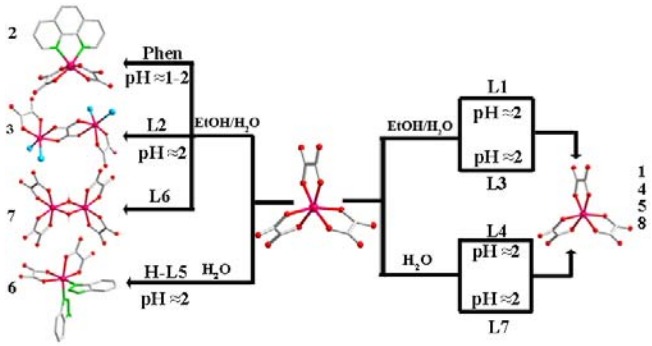

Scheme 3. The schematic representation of structural evolution of building-block in this work

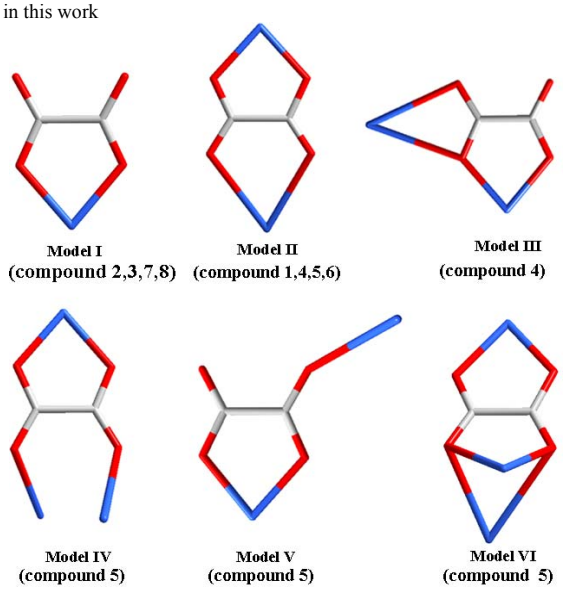

Crystal Structures. In the following, oxygen atoms of oxalate ligands are referred to as "internal" oxygen atoms when they are coordinated to iron, whereas those at the complex periphery are referred to as "external" oxygen atoms.The coordination modes of $C_2O_4^{2-}$ in complexes **1-8** are summarized in **Scheme 3**.

Structure of $[K(H\text{-}L_1)_2\{Fe(C_2O_4)_3\}\cdot 2H_2O]$ (1) Compound **1** crystallizes in the Orthorhombic system, space group *Ccca*, revealing a 3D H-bonded supramolecular architecture. As shown in Figure. 1a, its asymmetric unit consists of half a potassium cation, half a $[Fe(C_2O_4)_3]^{3-}$ anion, one $[H_2\text{-}L_1]^+$ cation and one H_2O molecule. Compound **1** has two different tetranuclear Fe_2K_2 rings, which alternate periodically within $[KFe(C_2O_4)_3]^{2-}$ layers (Figure. 1b-1c). Each $[Fe(C_2O_4)_3]^{3-}$ anion is linked to four K^+ cations and each dimeric potassium unit connects to six iron units. The oxalate ligands adopt two different coordination modes in compound **1**. The first one's carboxyl groups show μ_2-η^1:η^1 coordination mode (see Model II in Scheme 3), that is, oxalate ligands act as tetradentate ligands through internal oxygen atoms (namely, O1, O2, O5) toward the iron atom and external oxygen atoms (namely, O3, O4, O6) toward K1 with K(1)-O(3) = 2.853(2) Å, K(1)-O(4) = 2.698(2) Å, K(1)-O(6) = 3.0264(19) Å, respectively. The carboxyl groups of second one show μ_3-η^2:η^1 coordination mode (see Model VI). As a result, K1 adopts a distorted dodecahedron coordination geometry completed by eight oxygen atoms from four oxalate groups.

Discrete $[H\text{-}L_1]^+$ units and H_2O molecules are inserted between the adjoining $[KFe(C_2O_4)_3]^{2-}$ layers. The 2D $[KFe(C_2O_4)_3]^{2-}$ layers link the $[H\text{-}L_1]^+$ units and H_2O molecules to form a 3D supramolecular architecture (Figure. 1d). This association is accomplished through N1-H1···O1, N2-H2···O7 and O7-H7B···O6 H-bonds. Notably, H_2O molecules play a critical role for the formation of 3D H-bonded architecture, which is further stabilized by π-π interactions (d_{CC} = 3.49-3.55 Å) between the imidazole rings and the benzene rings.

Structure of $[(H\text{-}Phen)\{Fe(C_2O_4)_2(Phen)\}\cdot 3H_2O$ (2) Single-crystal X-ray diffraction analysis reveals that compound **2** crystallizes in the triclinic system, space group *P1*. As shown in Figure. 2a, its asymmetric unit is made up of one $[Fe(C_2O_4)_2(Phen)]^-$ anion, one $[H\text{-}Phen]^+$ cation, and three H_2O molecules. Each iron atom is coordinated by two nitrogen atoms from one Phen ligand as secondary building units and four oxygen atoms from two oxalate groups (adopt Model I) to furnish a distorted octahedral coordination geometry. The Fe-O bond lengths and Fe-N bond lengths (average values 1.9769 Å and 2.1529 Å, respectively) are close to that reported for iron(III) complexes containing Phen ligand and terminal oxalate ligand.[17] In compound **2**, a trimer water cluster is formed by means of O9-H9B···O10 and O11-H11B···O9 H-bonds, displaying a V-shaped structure (Figure 2b). Each $[Fe(C_2O_4)_2(Phen)]^-$ anion connects with four water molecules and the trimer water cluster connects four $[Fe(C_2O_4)_2(Phen)]^-$ anions by means of O···O H-bonds (O9-H9A···O7, O10-H10A···O3, O10-H10B···O2, O11-H11A···O7, O11-H11B···O9, and O11-H11A···O6 H-bonds), yielding a 2D network (Figure 2b), which contains seven-membered hydrogen-bonded rings of $[R^6_5(10)]$ and five-membered rings of $[R^5_3(17)]$. It is noted that the $[H\text{-}Phen]^+$ cations play the role of the pincers, which link the seven-membered hydrogen-bonded ring through N3-H3···O11 and C17-H···O2 H-bonds, giving rise to two different hydrogen-bonded rings [$R^4_5(7)$ and $R^5_5(9)$, respectively]. Furthermore, the adjoining 2D networks are mutual linked by the

CrystEngComm Accepted Manuscript

This journal is © The Royal Society of Chemistry 2012

Phen ligands and the $[H\text{-}Phen]^+$ cations to furnish a 3D architecture (Figure 2c-2d). This association is accomplished through H-bonds (N3-H3···O11, C7-H7···O5 and C17-H17···O2 H-bonds) and benzene rings π-π interactions (dcc = 3.60-3.75 Å).

CrystEngComm Accepted Manuscript

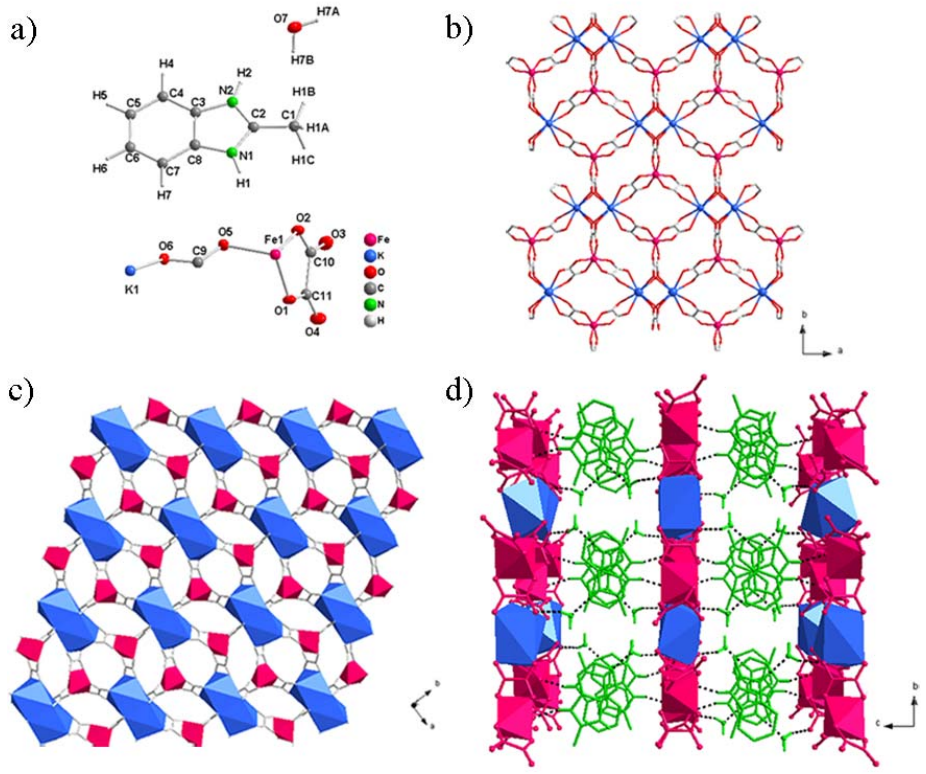

Figure 1. Structure of the $[K(H\text{-}L_1)_2\{Fe(C_2O_4)_3\}\cdot 2H_2O]$, **1**. (a) Molecular structure of **1** with atom labeling of the asymmetric unit. (b-c) 2D coordination networks developing in the *a,b* plan. (d) View of the 3D H-bonded architecture along the *a* axis. For the sake of clarity C-H H atoms are neglected in (d).

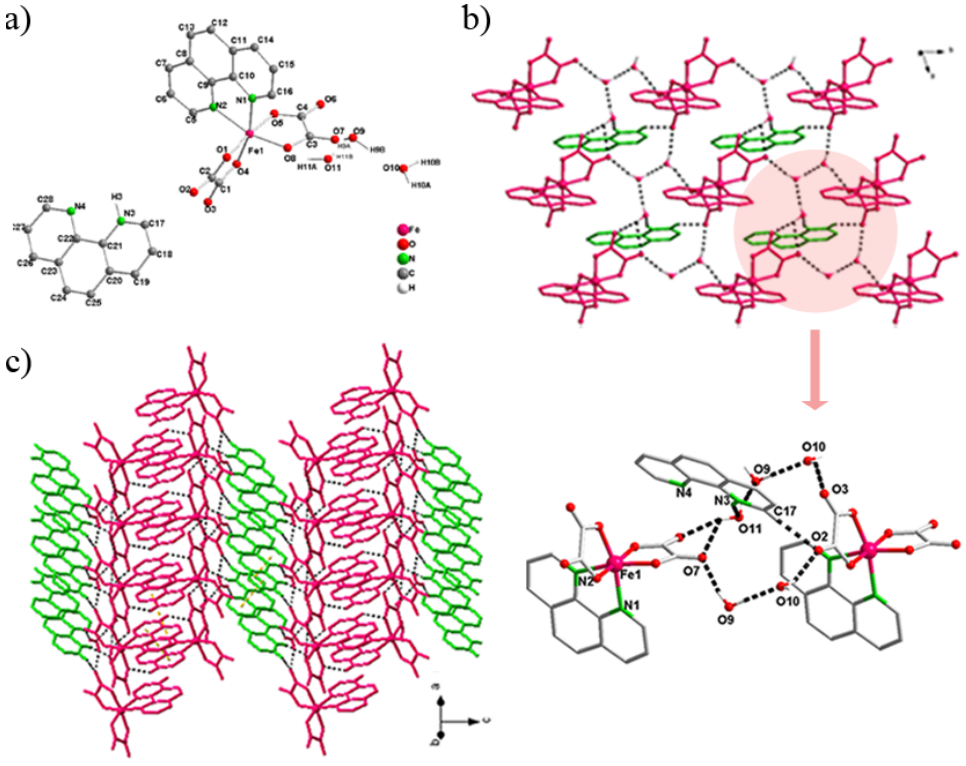

Figure 2. Structure of the $[(H\text{-}Phen)\{Fe(Phen)(C_2O_4)_2\}]\cdot 3H_2O$, **2**. (a) Molecular structure of **2** with atom labeling of the asymmetric unit. (b) 2-D network developing in the *a,b* plane. (c) View of the 3D H-bonded architecture along the *b* axis(c), the *(1,1,0)* direction. For the sake of clarity partial C–H H atoms are neglected in (a) (b), and (c).

CrystEngComm Accepted Manuscript

 This journal is © The Royal Society of Chemistry 2012

Structure of $[(H_2\text{-}L_2)_2\{Fe_2(C_2O_4)_3Cl_4\}]$ (3) L_2 ligand has appropriate size and degrees of freedom by means of free rotations around the C(sp3)-N(sp2) and C(sp2)-C(sp3) bonds. It was used to obtain distinct supramolecular architecture. Single-crystal X-ray diffraction analysis reveals that compound **3** crystallizes in the triclinic system, space group $P\bar{1}$. As shown in Figure. 3a, its asymmetric unit is made up by half a $[Fe_2(C_2O_4)_3Cl_4]^{4-}$ anion and halves of two different $[H_2\text{-}L_2]^{2+}$ cations. Each iron(III) atom is coordinated by two chlorine atoms and four oxygen atoms from two different oxalate ligands (adopt Model I and Model II coordination mode, respectively), resulting in a distorted octahedron. Two different $[H_2\text{-}L_2]^{2+}$ cations adopt trans-conformations. In the organic dications, the N4-C11-C11-N4 and the N2-C4-C4-N2 dihedral angle is 180°, and imidazolium-containing planes are parallel. A probable way to describe the 3D H-bonded networks of **3** is that the organic cations are linked to the binuclear $[Fe_2(C_2O_4)_3Cl_4]^{4-}$ units by means of N1-H1···O4, N3-H3···O4 and N3-H3···O5 H-bonds, leading to a 2D hydrogen-bonded network (Figure 3c). Although the hydrogen-bonded network frames with an opening of ca. 28 × 32 Å, the potential space is occupied by two same networks (Figure 3d). Those identical networks are further expanded into a close-packed 3D H-bonded architecture (Figure S1, Supporting Information) via weak C-H···O H-bonds (C4-H4B···O5 and C11-H···O6 H-bonds) and imidazole rings π-π interactions (dcc = 3.71 Å).

Structure of $[K(H_2\text{-}L_3)\{Fe(C_2O_4)_3\}\cdot 2H_2O]$ (4) $[H_2\text{-}L_2]^{2+}$ cations are replaced by methyl-substituted $[H_2\text{-}L_3]^{2+}$ cations, yielding a very different 3D H-bonded networks. Single-crystal X-ray diffraction analysis reveals that compound **4** crystallizes in the monoclinic system, space group *C2/c*. As shown in Figure. 4a Its asymmetric unit consist of half a K cation, half a $[Fe(C_2O_4)_3]^{3-}$, half a $[H_2\text{-}L_3]^{2+}$, and one H_2O molecule. Like for compound **3**, the $[H_2\text{-}L_3]^{2+}$ cations of **4** also adopt trans-conformations. In the $[H_2\text{-}L_3]^{2+}$ cations, the N2-C8-C8-N2 dihedral angle is 180° and imidazolium-containing planes are parallel. Each K ion is eight-coordinated with a distorted dodecahedron geometry, which is completed by six oxygen atoms afforded by three $[Fe(C_2O_4)_3]^{3-}$ units and two oxygen atoms from two water molecules. There are two different oxalate ligands within $[Fe(C_2O_4)_3]^{3-}$ units. The two carboxyl groups of one oxalate ligand adopt μ_2-η^2:η^1, μ_1-η^1:η^0 coordination modes (see Model III). However, the other one adopts Model II coordination mode. Therefore, potassium units of **4** are linked to $[Fe(C_2O_4)_3]^{3-}$ units yielding infinite ladder-like chains (Figure 4b), which are further extended into 2D network by the $[H_2\text{-}L_3]^{2+}$ cations (via N1-H1···O2 and N1-H1···O3 H-bonds; see Figure 4c). The dimensionality of architecture of **4** from 2D network to 3D architecture (Figure 4d) is achieved through C4-H4B···O3 and C6-H6···O6 H-bonds.

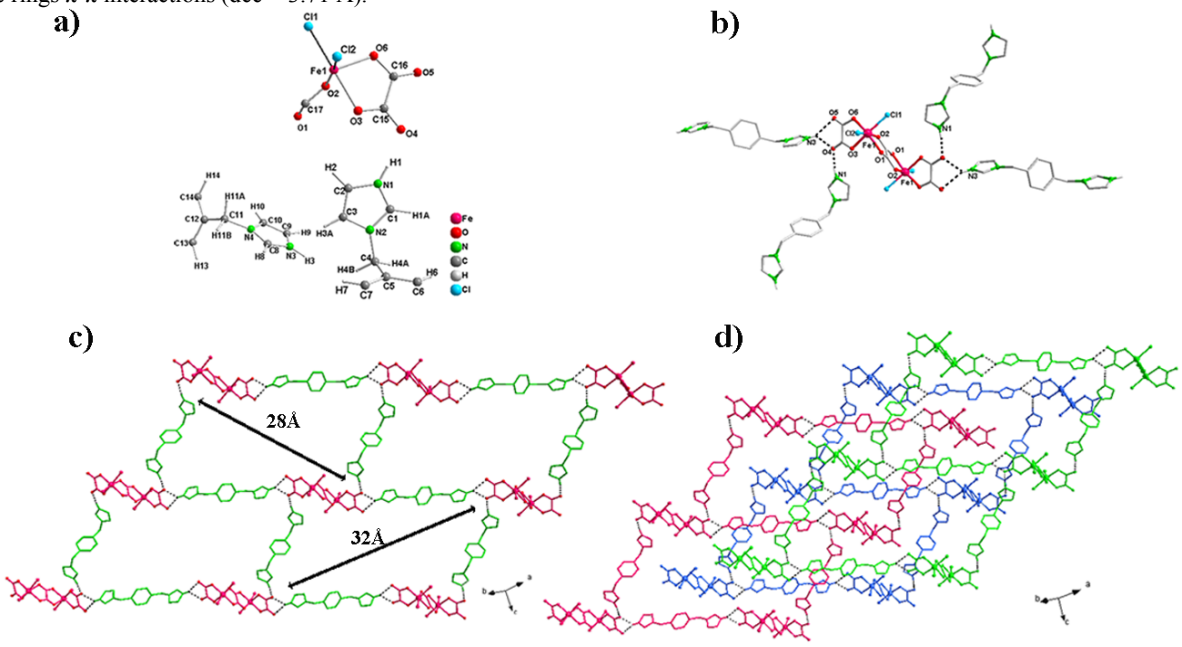

Figure 3. Structure of the $[(H_2\text{-}L_2)_2\{Fe_2(C_2O_4)_3Cl_4\}]$, **3**. (a) Molecular structure of **3** with atom labeling of the asymmetric unit (b) H-bonds between four $[H_2\text{-}L_2]^{2+}$ and one $[Fe_2(C_2O_4)_4Cl_2]^{4-}$ anion. (c) View of the 2-D H-bonded network of **3**. (c) The packing of three independent 2D networks (each independent 2D network is depicted with a different color).

Structure of $[K(H_2\text{-}L_4)\{Fe(C_2O_4)_3\}\cdot H_2O]$ (5) Compound **5** crystallizes in the monoclinic system, space group *C2/c*, revealing a 3D H-bonded supramolecular architecture. As shown in Figure. 5a, its asymmetric unit contains one K cation, halves of two different $[Fe(C_2O_4)_3]^{3-}$ anion, one $[H_2\text{-}L_4]^{2+}$ cation, and one H_2O molecule. The lattice water molecules ensure the cohesion of the crystal lattice. Similar to compound **1**, each $[Fe(C_2O_4)_3]^{3-}$ is linked to four K^+ cations and each dimeric potassium unit connects to six iron units. Oxalate ligands of the first $[Fe(C_2O_4)_3]^{3-}$ unit display Model II and Model VI coordination modes. Nonetheless, the oxalate ligands of the second $[Fe(C_2O_4)_3]^{3-}$ unit exhibit Model IV (the two carboxyl groups show the coordination modes μ_2-η^1:η^1 and μ_2-η^1:η^1) and Model V (the two carboxyl groups show the coordination modes μ_1-η^1:η^0

CrystEngComm Accepted Manuscript

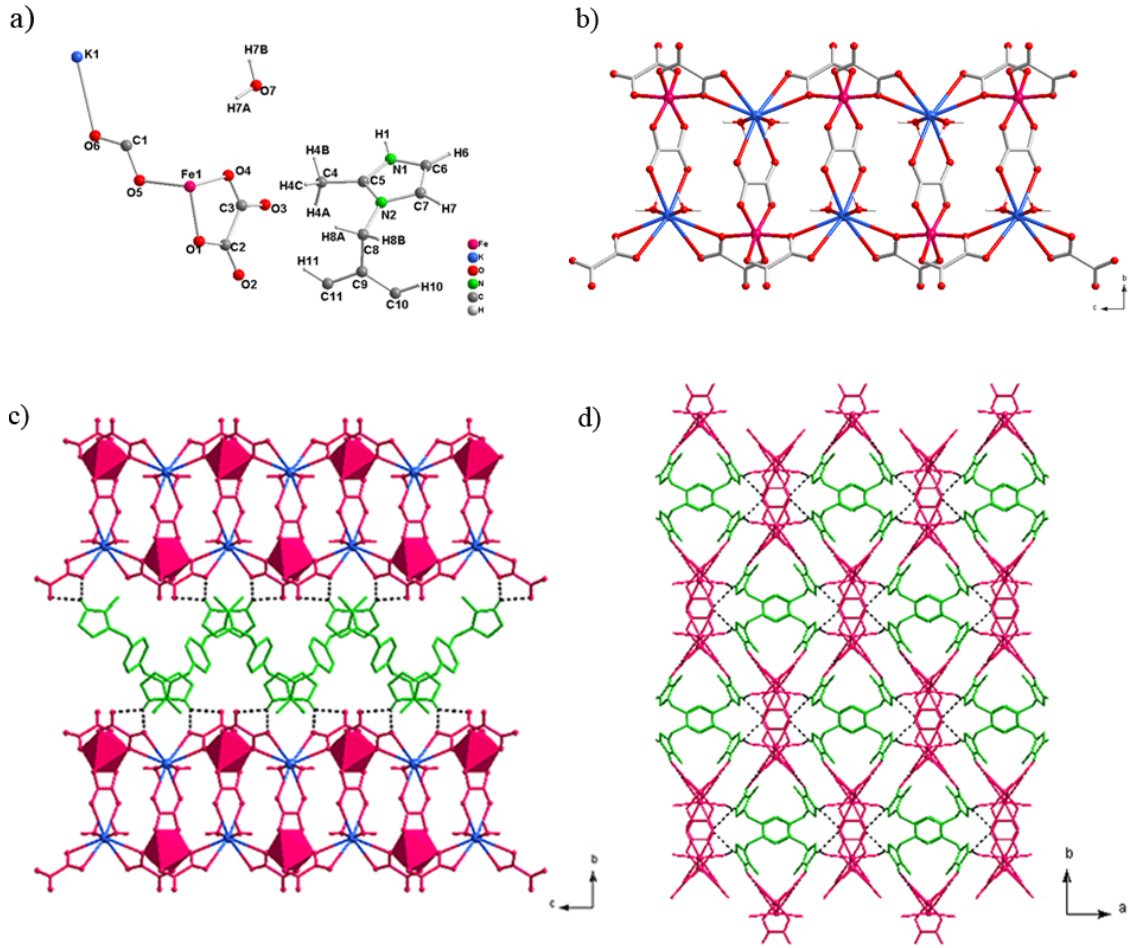

Figure 4. Structure of the $[K(H_2\text{-}L_3)\{Fe(C_2O_4)_3\}\cdot 2H_2O]$, **4**. (a) Molecular structure of **4** with atom labeling of the asymmetric unit. (b) The 1D ladder-like chain. (c) 2D networks developing in the *a,c* plan. (d) View of the 3D H-bonded architecture along the *c* axis. For the sake of clarity partial C−H H atoms are neglected in (c) and (d).

and μ_2-η^1:η^1) coordination modes. Hence, the $[KFe(C_2O_4)_3]^{2-}$ layer of **5** is different from the one of **1**. Each potassium atom of **5** is coordinated by six oxygen atoms from four $[Fe(C_2O_4)_3]^{3-}$ units and one oxygen atom from water molecules, showing a distorted pentagonal bipyramid geometry, which links another one by the edge-sharing of oxygen atoms. The discrete $[H_2\text{-}L_4]^{2+}$ units act as bridges, linking adjacent inorganic layers. In this way, the $[H_2\text{-}L_4]^{2+}$ units link the $[KFe(C_2O_4)_3]^{2-}$ layer to form a 3D supramolecular architecture, which is further stabilized by imidazole rings π-π interactions (d_{cc} = 3.47 Å; see Figure 5c). This association can be achieved via N-H···O hydrogen bonds (N1-H1···O2, N1-H1···O3, and N4-H4···O2 H-bonds) involving two outer oxygen atoms (namely O2, O3, respectively), and weak C-H···O hydrogen bonds (C7-H7···O12, and C16-H16···O7 H-bonds) involving all outer oxygen atoms and two inner oxygen atoms (namely, O5, O10, respectively).

Structure of $[(H\text{-}L_5)\{Fe(C_2O_4)\}(L_5)]$ (6) The X-ray crystallographic analysis reveals that compound **6** crystallizes in the monoclinic space group *Cc*. As shown in Figure. 6a The asymmetric structure is made up of one iron(III) ion, one L_5^- anion, one H-L_5 and one oxalate anion. Each iron(III) atom is coordinated by two nitrogen atoms from one H-L_5 ligand and one L_5^- anion (Fe-N = 2.144-2.172 Å), respectively, and four oxygen atoms from two oxalate groups (adopt Model II coordination modes; Fe-O = 2.137-2.186 Å), constructing a distorted octahedral environment. These units are mutually linked through the bis-bidentate oxalates, leading to an infinite 1D chain with a Fe···Fe separation of 5.5812 Å. Furthermore, the adjacent chains are connected by N4-H4···O1 and C5-H5···O2 H-bonds in three directions of space to form the resulting 3D supramolecular architecture (Figure 6c). The combination of Fe(III) and N-donor ancillary ligand depending on coordinate covalent bond is only found in compound **2** and **6**. It suggests that the N atoms of Phen and H-L_5 have stronger coordination ability than O atoms do.

Structure of $[\{(H_2\text{-}L_6)_2Fe_2(OH)_2(C_2O_4)_4\}\cdot 2H_2O]$ (7) Association between $[Fe(C_2O_4)_3]^{3-}$ and $[H_2\text{-}L_6]^{2+}$ yields **7**. Compound **7** crystallizes in the triclinic space group *P 1* , revealing a 3D H-bonded supramolecular architecture. Its asymmetric unit consists of half a $[Fe_2(OH)_2(C_2O_4)_4]^{4-}$, one $[H_2\text{-}L_6]^{2+}$, and one H_2O molecule (Figure S2, Supporting Information). The Fe-O bond lengths range from are 1.9883(19) to 2.0306 (18) Å, and O-Fe-O angles vary from 79.31(7) to 169.99(8)°. The characteristic of the Fe_2O_2 ring for the dimer is similar to those reported in analogous configurations[20]. In the binuclear $[Fe_2(C_2O_4)_4(OH)_2]^{4-}$ units (Figure 7a), Fe-O lengths to the bridging hydroxyl oxygen atoms are 1.9883(2) Å and 1.9951(2) Å, and

CrystEngComm Accepted Manuscript

 This journal is © The Royal Society of Chemistry 2012

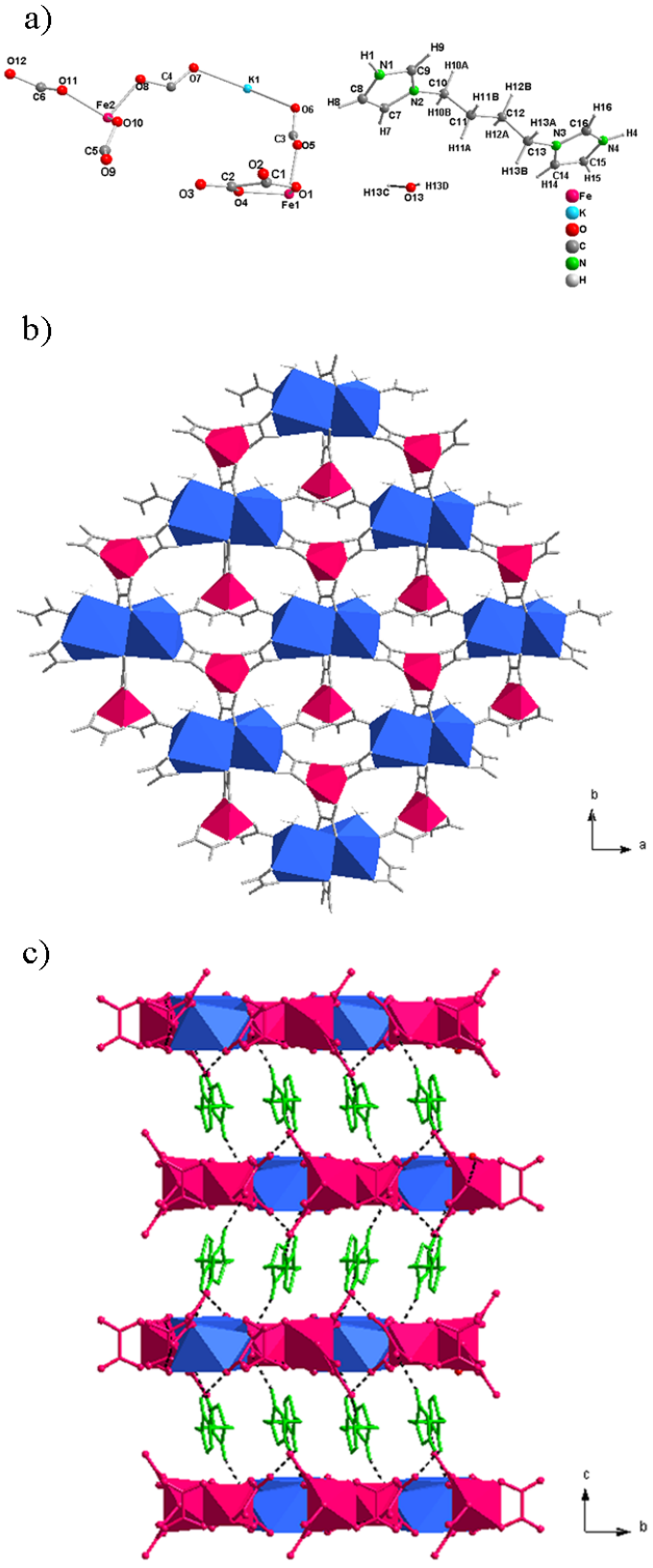

Figure 5. Structure of the $[K(H_2\text{-}L_4)\{Fe(C_2O_4)_3\}\cdot H_2O]$, **5**. (a) Molecular structure of **5** with atom labeling of the asymmetric unit. (b) 2D coordination networks developing in the *a,b* plan. (c) View of the 3D H-bonded architecture along the *a* axis. For the sake of clarity partial C–H H atoms are neglected in (c).

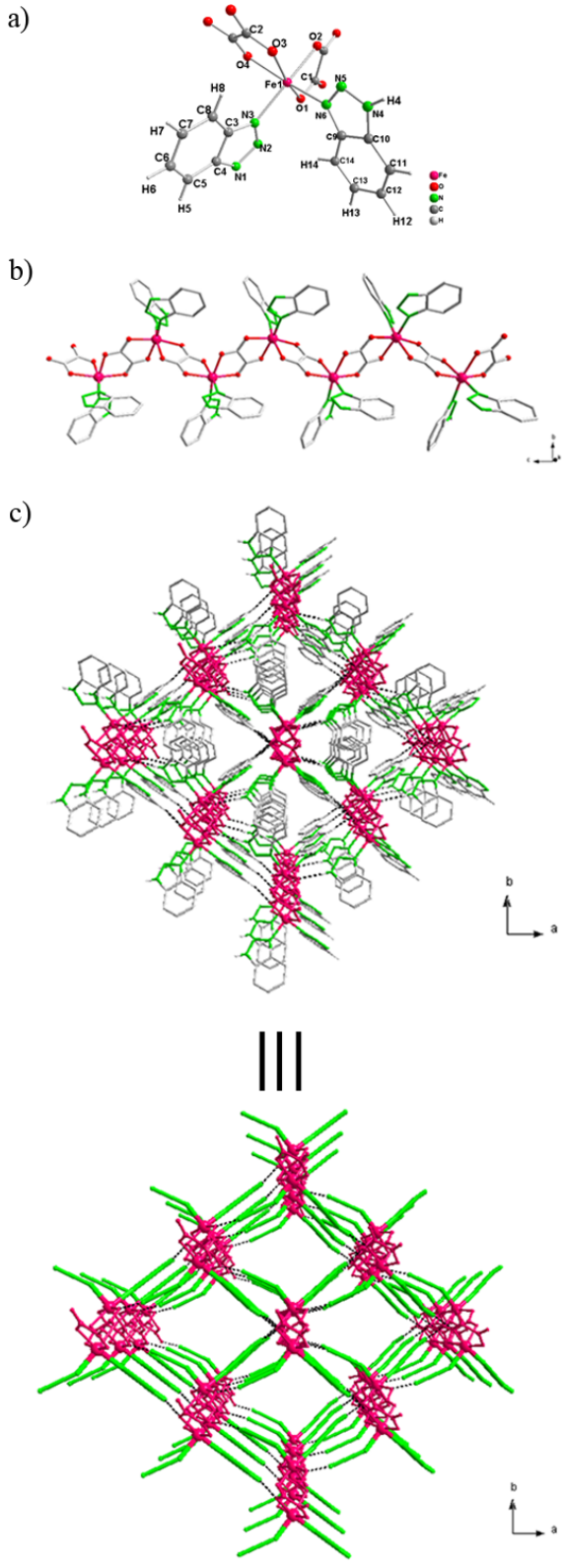

Figure 6. Structure of the $[(H\text{-}L_5)\{Fe(C_2O_4)\}(L_5)]$, **6**. (a) Molecular structure of **6** with atom labeling of the asymmetric unit. (b) View of the 1D chain of **6**. (c) View of the 3D H-bonded architecture along the *a* axis. For the sake of clarity C–H H atoms are neglected in (b) and partial C–H H atoms are neglected in (c).

CrystEngComm Accepted Manuscript

Fe-O-Fe angles are 100.45°(8). Furthermore, the adjacent Fe-Fe separations are 3.0615 Å(6). In compound **7**, each iron cation is coordinated by six oxygen atoms (four oxygen atoms from two oxalate groups adopted Mode I coordination mode, and two oxygen atoms from two hydroxyl groups), resulting in a distorted octahedron. Each $[Fe_2(OH)_2(C_2O_4)_4]^{4-}$ unit is associated to ten $[H_2\text{-}L_6]^{2+}$ cations through H-bonds involving three outer O-atoms (namely, O2, O3, O7, through N1-H1B···O2, N1-HB···O3, N1-H1C···O7, N2-H2A···O2, and N2-H2B···O3 H-bonds) and two inner O-atoms (namely, O1, O5, through N1-H1A···O5 and N2-H2A···O1 H-bonds; see Figure 7a), and each $[H_2\text{-}L_6]^{2+}$ cation connects to five $[Fe_2(C_2O_4)_4(OH)_2]^{4-}$ units, yielding a 3D supramolecular framework (Figure 7d).

Apart from the above associations, the adjoining $[Fe_2(C_2O_4)_4(OH)_2]^{4-}$ anions are mutually linked through O9-H9···O6 H-bonds, developing infinite chains (Figure 7b). These infinite chains are further connected by water molecules (through O10-H10A···O9 and O10-H10B···O8 H-bonds, respectively; Figure7c) to construct a resulting 2D H-bonded network.

Structure of $[(H_2\text{-}L_7)_4\{Fe(C_2O_4)_3\}Cl\cdot 2H_2O]$ (8) Association between $[Fe(C_2O_4)_3]^{3-}$ and $[H\text{-}L_7]^{+}$ yields **8**. Single-crystal X-ray diffraction analysis reveals that compound 8 crystallizes in the monoclinic system, space group *P2(1)/c*, showing a 3D H-bonded architecture. As shown in Figure. 7a, its asymmetric unit consists of one $[Fe(C_2O_4)_3]^{3-}$ anion, four $[H\text{-}L_7]^{+}$ cation, one Cl^- and two water molecules. In this compound, each $[Fe(C_2O_4)_3]^{3-}$ unit connects ten $[H\text{-}L_7]^{+}$ cations that act as the bridge among different metallotectons through all outer O-atoms (namely, O2, O3, O6, O7, O10 and O11, via N14-H14···O2, N16-H16B···O3, N5-H5A···O6, N23-H23B···O6, N21-H21···O7, N24-H24B···O7, N22-H22B···O10, N4-H4B···O11 and N22-H22A···O11 H-bonds) and five inner O-atoms (namely, O4 ,O5, O8, O9 and O12, through N24-H24B···O4, N9- H9···O5, N6-H6B···O8, N21-H21···O9, N10-H10B···O12 H-bonds; see Figure S3, Supporting Information) to furnish a closed 3D H-bonded framework (Figure S4, Supporting Information). Differing from other compounds, trinary hydrogen bonds and doubly hydrogen bonds are simultaneously displayed in this aggregate.

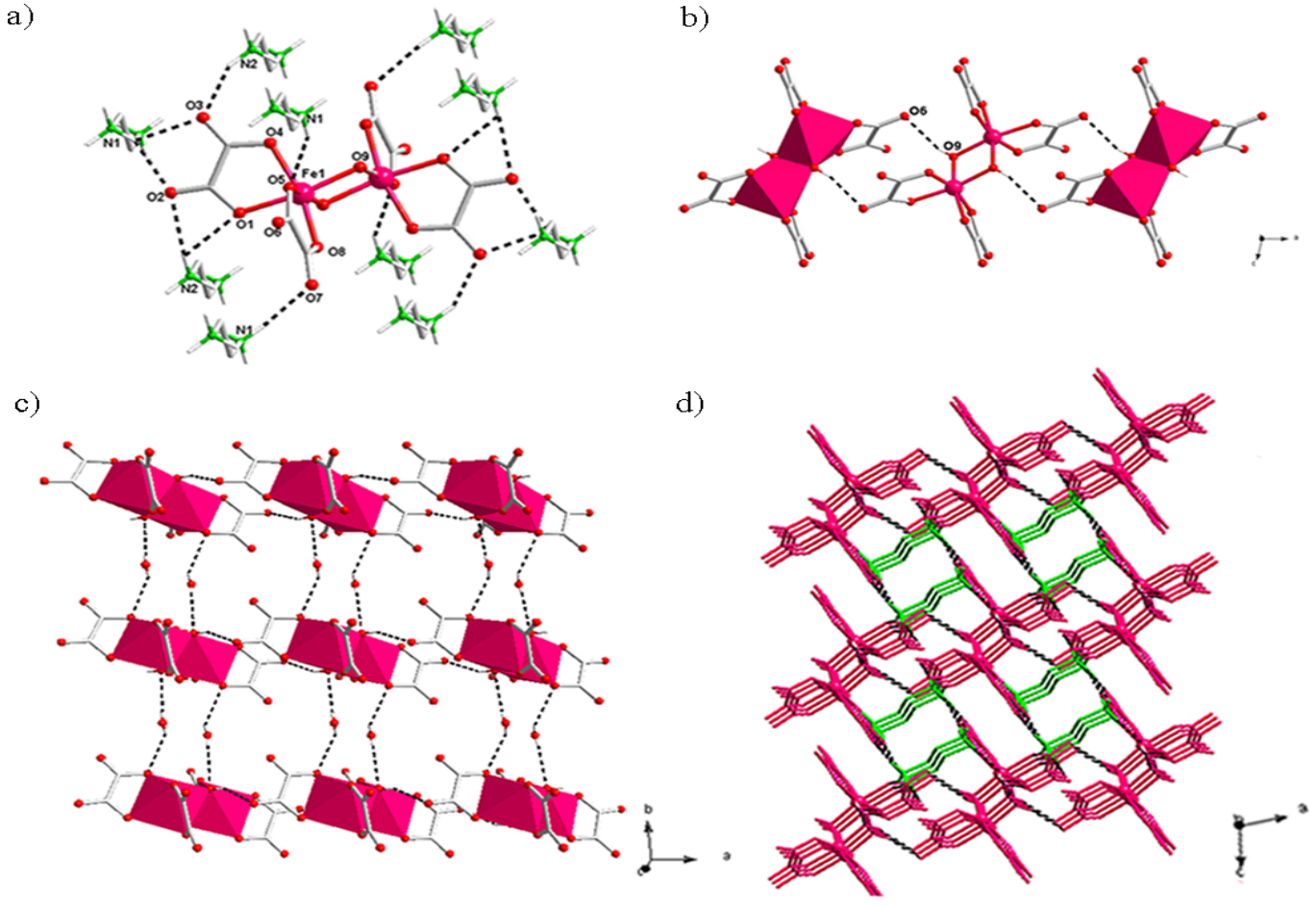

Figure 7. Structure of $[\{(H_2\text{-}L_6)_2Fe_2(C_2O_4)_4(OH)_2\}\cdot 2H_2O]$, **7**. (a) Detail of the connection between ten $[H2\text{-}L_6]^{2+}$ and one $[Fe_2(OH)_2(C_2O_4)_4]^{4-}$ anion. (b) 1D supramolecular chains ruining along the *b* axis.(c) 2-D network developing in the *a,b* plane. (d) View of the 3D H-bonded architecture along the *b* axis. For the sake of clarity partial C–H H atoms are neglected in (a) and (d).

CrystEngComm Accepted Manuscript

This journal is © The Royal Society of Chemistry 2012

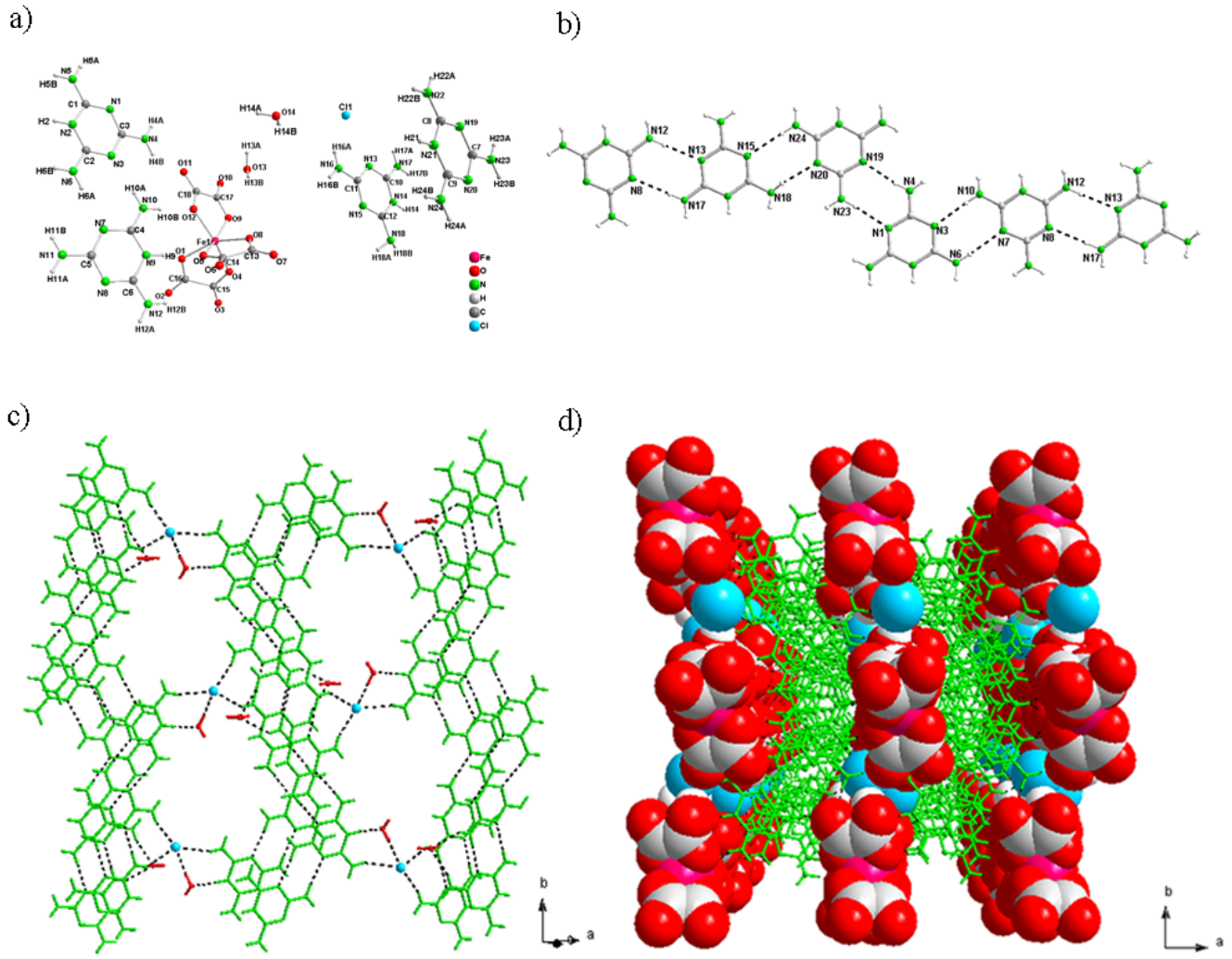

Figure 8. Structure of the $[(H\text{-}L_7)_4Fe(C_2O_4)_3Cl{\cdot}2H_2O]$, **8. (a)** Molecular structure of **8** with atom labeling of the asymmetric unit. (b) The 1D H-bonded chain. (c) View of the 2D network along *z* axis (d) View of the 3D (Fe^{3+}, $C_2O_4^{2-}$ and Cl^- are adopted space-filling model) architecture of **8**.

$[H\text{-}L_7]^+$ are sequentially assembled by means of four pairs of double hydrogen bonds, which both in a $[R_2^2(6)]$ pattern, to form polymeric ribbonlike 1D supramolecular aggregates. H_2O molecules are located in channels between adjacent 1D aggregates. Although compound **8** has displayed a 3D structure based on the $[Fe(C_2O_4)_3]^{3-}$ anions and $[H\text{-}L_7]^+$ cations through H-bonds, the chlorine anion also plays a vital role to sustain the 3D network (via N-H···Cl and O-H···Cl H-bonds; see Figure 8c-8d). In other words, the adjoining 1D aggregates of $[H\text{-}L_7]^+$ are connected by Cl^- to generate a 2D network. In compound **8**, π-π interactions (d_{CC} = 2.86 - 3.83 Å) are also observed between the $[H\text{-}L_7]^+$ cations. However, the incorporation of the chlorine anion is observed only in compound **3** and **8**, and the potassium cation is observed in compound **1 4** and **5**. In fact, the reason can't be elucidated clearly for the moment, perhaps the stoechiometry of final compound can be regarded as a main factor.

Thermogravimetric Analysis.

The thermogravimetric (TG) analyses of compounds **1**−**8** have been performed in the temperature range of 35−900 °C under N_2 atmosphere with a heating rate of 10 °C·min^{-1} (Figure 9 and Figure S5, Support information). Results of the TGA curves of **1-8** suggest that their host frameworks were stable up to ~230, ~270, ~210, ~250, ~, 320, ~190, ~180, and ~220°C, respectively. Then the networks begin to collapse. The TG curves of compounds **2** and **5-8** show two weight loss steps. The release of water molecules can be observed with the weight loss of 6.9% (calcd 8.3% for **2**), 3.2 % (calcd 3.1% for **5**), 7.1% (calcd 5.5% for **7**), 3.8% (calcd 3.5% for **8)**, respectively. The residual weight is 21.97% (calcd for Fe_2O_3, 24.7%) for **2**, 25.2% (calcd for Fe_2O_3, 28.1%) for **5**, 41.45% (calcd for Fe_2O_3, 42.0%) for **6**, 25.75% (calcd for Fe_2O_3, 24.3%) for **7**, 10 45% (calcd for Fe_2O_3, 17.7%) for **8**. However, compound **1**, **3** and **4** possess three weight loss steps. For **1**, the first weight loss between 150-205°C is attributed

CrystEngComm Accepted Manuscript

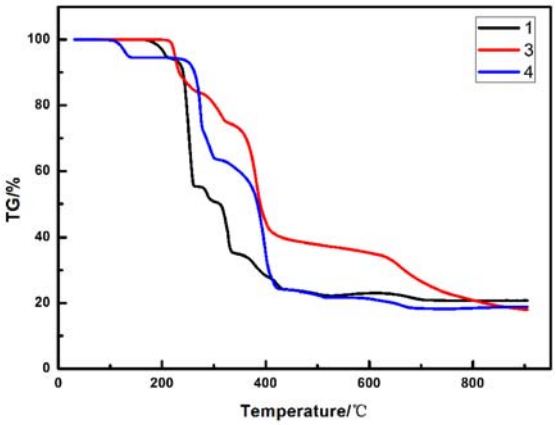

Figure 9. Thermogravimetric analyses (TGA) curves of **1**, **3** and **4.**

to the lost of uncoordinated water molecules (obsd 5.1%, calcd 4.8 %). The further weight lost between 230-260°C corresponding to the loss of oxalate ligands (obsd 39.7%, calcd 39.9 %). Above 280°C, it starts to lose its N-donor ligands a result of thermal decomposition. Compound **3** shows the first mass weight loss of 25.0% below 320°C is attributed to the decomposition of oxalate ligands (calcd 26.4%). The weight loss occurring between 320-560°C (38.8%) is attributed to the decomposition of N-donor ligands (calcd 47.8%). Moreover, the third weight loss of 13.9% from 590-800°C should be attributed to the release of coordinated chloride ion (calcd 14.2%). Compound **4** shows the first weight loss of 5.4% below 145°C due to the removal of water molecules (calcd 5.4%). The second weight loss of 32% occurring between 250-300°C is attributed to the decomposition of oxalate ligands (calcd 39.7%). The N-donor ligands begin to decompose at 310°C. The residual weight is 22.8% (calcd for Fe_2O_3, 24.1%) for **1**, 21.7% (calcd for Fe_2O_3, 16.0%) for **3**, 21.7% (calcd for Fe_2O_3, 24.1%) for **4**.

Conclusions

We have successfully synthesized a series of 3D iron-organic supramolecular materials with modest thermal stability by association of $[Fe(C_2O_4)_3]^{3-}$ as hydrogen-bond acceptor and organic cations as hydrogen-bond donors. Using preformed metal-organic compounds as building units may be utilized as the simplest possible and efficient tool for constructing predictable structure from different discrete molecular. Structural comparisons indicate that the resulting H-bonded framework strongly depends on the nature of the ligand. The bonding strength between the building-blocks is reinforced by N-donor ancillary ligands with six or eight available hydrogen atoms. Apparently, those N-donor groups seem to result in rather compact assemblages. In addition, the weak interactions (π···π interactions and C–H···O H-bonds) will play a crucial role if the stronger H-bonds are utilized and quenched. The secondary ligand containing unprotonated N atoms are likely to replace the water molecules of $[Fe(C_2O_4)_2{\cdot}(H_2O)_2]^-$ to complete the coordination geometry of Fe(III), leading to the diversity of H-bonded frameworks. Employing this synthetic route, we have prepared a lot of new hybrid supramolecular materials that will be reported in future papers.

Acknowledgements

This work was supported by the National Natural Science Foundation of China (No. 51372125, 21176128 and 21203106), the Natural Science Foundation of Shandong Province, China (No. ZR2011BL015), and the State Key Laboratory of Inorganic Synthesis and Preparative Chemistry (2013-34).

References

1 (a) G. R. Desiraju, *Angew. Chem.*, *Int. Ed*. 2007, **46**, 8342-8356; (b) G. R. Desiraju, *Chem. Commun.*, 1997, **16**, 1475-1482; (c) L. Brammer, *Chem. Soc. Rev*., 2004, **33**, 476-489.

2 (a) W. Wei, M. Y. Wu, Q. Gao, Q. F. Zhang, Y. G. Huang, F. L. Jiang, M. C. Hong, *Inorg. Chem.*, 2009, **48**, 420-422; (b) C. Zhao, Q. F. Sun, W. M. Hart-Cooper, A. G. DiPasquale, F. D. Toste, R. G. Bergman, K. N. Raymond, *J. Am. Chem. Soc*., 2013, **135**, 18802-18805; (c) R. Bishop, *Acc. Chem. Res*., 2009, **42**, 67-78.

3 (a) W. Wei, M. Y. Wu, Q. Gao, Q. F. Zhang, Y. G. Huang, F. L. Jiang, M. C. Hong, *Inorg. Chem.*, 2009, **48**, 420-422; (b) C. Zhao, Q. F. Sun, W. M. Hart-Cooper, A. G. DiPasquale, F. D. Toste, R. G. Bergman, K. N. Raymond, *J. Am. Chem. Soc*., 2013, **135**, 18802-18805; (c) R. Bishop, *Acc. Chem. Res*., 2009, **42**, 67-78.(d) L. Wang, L. Zhao, Y. J. Hu, W. Q. Wang, R. X. Chen, Y. Yang, *CrystEngComm*., 2013, **15**, 2835-2852; (d) C. M. Jr, M. T Pope, S. O'Donnell, *Inorg. Chem.,* 1974, **4**, 831-833.

4 (a) K. Sekizawa, K. Maeda, K. Domen, K. Koike, O. Ishitani, *J. Am. Chem. Soc*., 2013, **135**, 4596-4599; (b) L. H. Wang, R. Shang, Z. Zheng, C. L. Liu, Z. M. Wang, *Cryst. Growth Des*., 2013, **13**, 2597-2606.

5 (a) I. Imaz, A. Thillet, J. P. Sutter, *Cryst. Growth Des*., 2007, **7**, 1753-1761; (b) F. Thétiot, C. Duhayon, T. S. Venkatakrishnan, J. P. Sutter, *Cryst. Growth Des*., 2008, **8**, 1870-1877; (c) H. E. Bakkali, A. Castiñeiras, I. García-Santos, J. M. González-Pérez, J. N. Niclós-Gutiérrez, *Cryst. Growth Des*., 2014, **14,** 249-260.

6 (a)X. Shi, G. Zhu, X. Wang, G. Li, Q. Fang, G. Wu, G. Tian, M. Xue, X. Zhao, R. Wang, S. Qiu, .*Cryst. Growth Des*., 2005, **5**, 207-213; (b) X. Shi, G. Zhu, X. Wang, G. Li, Q. Fang, X. Zhao, G. Wu, G. Tian, M. Xue, R. Wang, S. Qiu, *Cryst. Growth Des*., 2005, **5**, 342-346.

7 (a) Y. Wang, J. Yu, M. Guo, R. Xu, *Angew. Chem.*, *Int. Ed*. 2003, 34, 4089-4092; (b) J. Yu, Y. Wang, Z. Shi, R. Xu, *Chem. Mater*. 2001, **13**, 2972-2978.

8 (a) I. Imaz, G. Bravic, J. P. Sutter, *Dalton Trans*., 2005, **16**, 2681-2687; (b) I. Imaz, G. Bravic, J. P. Sutter, *Chem. Commun*., 2005, **8**, 993-995.

9 G. Mouchaham, R. Nans, S. Brandès, C. Duhayon, J. P. Sutter, *Cryst. Growth Des*., 2011, **11**, 5424-5433.

10 (a) S. Xu, C. M. Hessel, H. Ren, R. B. Yu, Q. Jin, M. Yang, H. J, Zhao, D. Wang, *Energy Environ. Sci.,* 2014, **7**, 632-637; (b)

CrystEngComm Accepted Manuscript

 This journal is © The Royal Society of Chemistry 2012

Z. M. Li, X. Y. Lai, H. Wang, D. Mao, C. J. Xing, D. Wang, *Nanotechnology.,* 2009, **20**, 245603; (c) R. B. Yu, X. R. Xing, T. Saito, M. Azuma, M. Takano, D. Wang, Y. F. Chen, N. Kumada, N. Kinomura, *Solid State Science.,* 2005, 7, 221-226; (d) D. Wang, R. B. Yu, X. R.Xing, Y. F. Chen, Z. C. Guo, N. Kumada, N. Kinomura, M, Takano, *Solid State Science.,* 2004, **175**, 751-754; (e) R. B. Yu, D. Wang, Y. F. Chen, X. R. Xing, S. Ishiwata, T. Saito, M. Takano, *Chemistry Letters.,* 2004, **33**, 1186-1187; (f) R. B. Yu, D. Wang, S. Ishiwata, T. Saito, M. Azuma, M. Takano, Y. F. Chen, J. H.Li, *Chemistry Letters.,* 2004, **33**, 458-459; (g) A. Duong, T. Maris, J. D. Wuest, *Inorg. Chem*., 2011, **50**, 5605-5618; (h) C. Q. Wan, G. S. Li, X. D. Chen,C. W. T. Mak, *Cryst. Growth Des*., 2008, **8**, 3897-3901; (i) J. W. Leeland, F. J. White, J. B. Love, *J. Am. Chem. Soc*., 2011, **133**, 7320-7323; (j) E. Cariati, R. Mcchi, D. Roberto, R. Ugo, S. Galli, N. Casati, P. Macchi, A. Sironi, L. Bogani, A. Caneschi, D. Gatteschi, *J. Am. Chem. Soc*., 2007, **129**, 9410-9420.

11 (a) M. Sadakiyo, H. Okawa, A. Shigematsu, M. Ohba, Y. Yamada, H. Kitagawa, *J. Am. Chem. Soc*., 2012, **134**, 5472-5475; (b) M. Sadakiyo, Y. Yamada, H. Kitagawa, *J. Am. Chem. Soc*., 2009, **131**, 9906-9907; (c) T. G. Prokhorova, L. I. Buravov, E. B. Yagubskii, L. V. Zorina, S. S. Khasanov, S. V. Simonov, R. P. Shibaeva, A. V. Korobenko, V. N. Zverev, *CrystEngComm*., 2011, **13**, 537-545.

12 (a) L. Martin, S. S. Turner, P. Day, P. Guionneau, J. A. K. Howard, D. E. Hibbs, M. E. Light, M. B. Hursthouse, M. Uruichi, K. Yakushi, *Inorg. Chem*., 2001, **40***,* 1363-1371; (b) S. Rashid, S. S. Turner, P. Day, M. E. Light, M. B. Hursthouse, *Inorg. Chem*., 2000, **39***,* 2426-2428.

13 J. P. García-Terán, O. Castillo, A. Luque, U. García-Couceiro, G. Beobide, P. Román, *Inorg. Chem*., 2007, **46**, 3593-3602.

14 X. Yang, J. Li, X. H. Zhao, H. W. Wang, Y. K. Shan, *Acta Cryst*., 2007, **C63**, m171-m173.

15 S. Decurtins, H. W. Schmalle, P. Schneuwly, H. R. Oswald, *Inorg. Chem*., 1993, **32***,* 1888-1892.

16 E. Cariati, R. Macchi, E. Tordin, R. Ugo, L. Bogani, A. Caneschi, P. Macchi, N. Casati, A. Sironi, *Inorg. Chim. Acta*.,2008, **361**, 4004-4011.

17 D. Armentano, G. D. Munno, F. Lloret, M. Julve, *CrystEngComm.*, 2005, **7**, 57-66.

18 C. Maxim, S. Ferlay, C. Train, *New. J. Chem*., 2011, **35**, 1254-1259.

19 G. M. Sheldrick, SHELXS-97 and SHELXL-97; Bruker AXS Inc.: Madison, WI, 2000.

20 A. S. Attia,, B. J. Conklin, C. W. Lange, C. G. Pierpont, *Inorg. Chem*., 1996, **35**, 1033-1038.

1

CrystEngComm Accepted Manuscript